

# Modeling and Analysis of Bi-connected Minimum Energy Path Preserving Graphs for Wireless Multi-hop Networks

Ashikur Rahman  
Dept. of Comp. Sci. & Engg. (CSE)  
Bangladesh Univ. of Engg. & Tech. (BUET)  
Dhaka-1000, Bangladesh  
ashikur@cse.buet.ac.bd

Raqeebir Rab  
Dept. of Comp. Sci. & Soft. Engg (CSSE)  
Concordia University  
Montreal, Canada, H3G 1M8  
r\_rab@encs.concordia.ca

## ABSTRACT

Topology control (TC) algorithms in wireless multi-hop networks create connected communication subgraphs that satisfy some desirable topological properties such as minimum-energy, fault tolerance, minimum interference, and bounded node degree. However, preserving two or more combination of these properties simultaneously is harder to achieve and often overlooked by the research community. In this paper, we describe a connectivity preserving topology control algorithm which combines two important properties, e.g., (a) minimum energy, and (b) fault tolerance. For the topology generated by the algorithm, we provide an analytical model to estimate its structural density. The accuracy of the analytical model is validated with extensive simulation results.

## Categories and Subject Descriptors

C.2.1 [Computer-Communication Networks]: Network Architecture and Design—*Network topology*

## General Terms

Algorithms, Performance, Verification

## Keywords

Fault tolerance; Topology control; Graph; Biconnectivity; Energy; Modeling; Wireless multihop networks

## 1. INTRODUCTION

Wireless multi-hop networking is known as the *art of networking without a network*. Large-scale wireless sensor networks—a special kind of multi-hop networks—have gained popularity in a wide range of mission-critical situations due to their cost-effectiveness, potential benefits and ease of deployment. Creating fault-tolerant dynamic topologies is one of the major challenges in the design of such mission-oriented sensor networks.

Topology control (TC) algorithms [10, 6, 9, 17] in all types of wireless multi-hop networks determine a connected communication subgraph that satisfies some topological properties by finding

Permission to make digital or hard copies of all or part of this work for personal or classroom use is granted without fee provided that copies are not made or distributed for profit or commercial advantage and that copies bear this notice and the full citation on the first page. Copyrights for components of this work owned by others than ACM must be honored. Abstracting with credit is permitted. To copy otherwise, to republish, to post on servers or to redistribute to lists, requires prior specific permission and/or a fee. Request permissions from permissions@acm.org.

MiSeNet'13, October 4, 2013, Miami, Florida, USA

Copyright 2013 ACM 978-1-4503-2367-3/13/10 ...\$15.00.

http://dx.doi.org/10.1145/2509338.2509343.

appropriate transmission power assignment of each node. Some of the properties that are considered by a vast majority of researchers include minimum-energy, fault tolerance, minimum-interference, and load balancing, to name a few. However, preserving two or more combination of these properties is harder to achieve and often overlooked by the research community. For example, a topology control algorithm may combine fault tolerance with the minimum energy property by generating a  $k$ -connected communication (sub)graph that preserves all minimum energy paths between every pair of nodes. Creating topologies in this way has an obvious advantage of transmitting over the minimum energy path at first place and maintaining connectivity through another backup path in case of node failure(s) or departure(s) on the minimum energy path.

In this paper, we discuss a fault-tolerant minimum-energy path-preserving topology control algorithm and provide mathematical analysis to derive its key performance metric called *sparseness*. Sparseness is formally defined as the average number of nodes located within the transmission range of a node. In wireless multihop networks, each node is connected with all its neighbours through direct (sort of virtual) links. Consequently, sparser networks have fewer links on the average and are more preferable as a network with more links is subject to more contentions, interferences and packet losses. Thus, sparseness is a key metric in comparing topologies generated from different topology control protocols.

## 1.1 Formal description of the problem

Consider an  $n$ -node, mission-oriented wireless sensor network deployed on a two-dimensional plane. Let us assume that the set of nodes, each equipped with a radio transceiver, is denoted by  $V = \{t_1, t_2, \dots, t_n\}$ . Suppose the transmission power  $p(t)$  of any node  $t$  is adjustable up to a maximum amount  $P_{max}$ , i.e.,  $0 \leq p(t) \leq P_{max}$ . Such a network can be modeled as a graph  $G_{max} = (V_{max}, E_{max})$ , with the vertex set  $V_{max}$  representing the nodes, and the edge set  $E_{max}$  defined as follows:

$$E_{max} = \{(s, t) | (s, t) \in V \times V \wedge d(s, t) \leq R_{max}\} \quad (1)$$

where  $d(s, t)$  is the distance between nodes  $s$  and  $t$  and  $R_{max}$  is the maximum distance reachable by using transmission power  $P_{max}$ . The graph  $G_{max}$  is often called the *maximum powered network*.

It is customary to assume that the minimum transmission power required to transmit to distance  $d$  is proportional to  $d^\alpha$  where  $\alpha$  is the well-known path loss factor [16]. Thus node  $t$  receives transmission from  $s$  if  $p(s) \geq K \times d^\alpha(s, t)$ , for some constant  $K$ . A power assignment  $\hat{p}$  of  $V$  is a vector of transmission powers, i.e.,  $\hat{p} = \{p(t) | t \in V\}$ . The transmission possibilities resulting from a power assignment induce a subgraph  $G' = (V, E')$  of  $G_{max}$ , where  $E' = \{(s, t) | p(s) \geq K \times d^\alpha(s, t)\}$  is the set of directed edges resulting from the power assignment.

**Table 1: Summary of Notations**

Notation	Description
$G_{max}$	Maximum powered graph
$R$	Transmission radius
$r, s, t, u, v, w$	Nodes in a wireless ad hoc network
$(s, t)$	A node pair
$\langle s, t \rangle$	An edge between nodes $s$ and $t$
$\langle x, y \rangle$	Physical location of a node
$d(s, t)$	Distance between a node pair $(s, t)$
$\alpha$	Path loss factor
$K$	Global constant in path loss model
$P_{s \rightarrow t}$	Transmission power required to send from $s$ to $t$
$P_{s \rightarrow r \rightarrow t}$	Transmission power required to send from $s$ to $t$ using a node $r$ as a relay
$C_{(s,t)}$	Cover region of $(s, t)$ node pair
$\xi_G(s, t)$	Cover set of $(s, t)$ node pair
$T_e$	Expected number of neighbors eliminated
$F_e$	Fraction of neighbors eliminated

One of the interesting fundamental problems in mission-oriented wireless sensor networks is to find a power assignment which induces a communication subgraph of  $G_{max}$  and satisfies some topological properties. One can envision a number of such (interesting) topological properties such as planarity, bounded node degree, minimum-interference etc. However, in this paper we limit ourselves in two of such properties namely: i) *minimum energy property*, and ii) *bi-connectivity*. An induced subgraph  $G'$  is said to hold minimum energy property if for any node pair  $s$  and  $t$  the minimum energy path between  $s$  and  $t$  in  $G_{max}$  is also preserved in  $G'$ . On the other hand the induced subgraph  $G'$  holds bi-connectivity property if the connectivity still holds on the subgraph derived from  $G'$  after removing any single node. Note that when a graph holds both biconnectivity and the minimum energy property together then there exist at least two vertex disjoint paths between every pair of nodes  $u$  and  $v$  in  $G'$  and in addition to that the minimum energy paths between every node pairs are preserved. Controlling topology in this way has a benefit of maintaining connectivity through another backup path making the topology more resilient to any node failures or departures.

In one of our previous works [18], we have proposed a distributed algorithm to find a suitable power assignment for constructing a graph  $G_b \subseteq G_{max}$  based on local information (i.e. one hop neighbour information) so that for the induced subgraph  $G_b$ : (i) the minimum energy property is preserved, and (ii) strong connectivity is 2-fault resilient in  $G_b$ . However, no insight or mathematical models were provided to determine sparseness generated from the algorithm. Thus, we seek to fill this notable gap by developing mathematical models to estimate sparseness from the network parameters such as node density, and transmission ranges.

In the rest of the paper, we present the formal definition of minimum energy path-preserving biconnected topologies, analyze their structural properties, and discuss their performance trade-offs. In particular, Section 2 provides a brief discussion of prior related research works. Section 3 presents a distributed fault tolerant topology control algorithm, and provides some fundamental bounds. Section 4 develops the analytical model to characterize the structure of minimum energy path preserving biconnected topologies, while Section 5 presents simulation results to validate our model. Finally, Section 6 concludes the paper with some pointers to pos-

sible future works. Table 1 provides a summary of the notational conventions used in our analysis.

## 2. RELATED WORK

In this section, we review power-aware topology control algorithms for wireless ad hoc networks. All research works found in the literature can be broadly classified into three groups.

The first class of solutions looks at the issue from the perspective of the MAC layer. Monks *et al.* [13] propose a modification of the RTS-CTS handshake mechanism in IEEE 802.11 [4] that can lead to energy savings. They develop a technique based on estimating a receiver's distance from the perceived signal strength of the CTS packets sent by the receiver. Once the distance is estimated, the sender re-adjusts its transmission power for subsequent data transmissions to an appropriate level strong enough to reach the destination. Singh *et al.* [20] propose powering-off transceivers to reduce energy consumption when they are not actively transmitting or receiving any packets.

The second approach, known as *power-aware routing*, combines power savings with routing. Most of the schemes in this class use distributed variants of the Bellman-Ford algorithm, but with cost metrics related to power. Some of these metrics are energy consumed per packet, time to network partition, variance in node power levels, and (power) cost per packet [21].

The third approach, which mostly matches with ours, separates routing from topology control, although power-aware routing protocols are often used in conjunction with solutions in this class. Some of the most notable contributions in this category are described next.

Ramanathan *et al.* [15] describe two centralized algorithms to minimize the maximum transmission power used by any node while maintaining connectivity or bi-connectivity. Two distributed heuristics called Local Information No Topology (LINT) and Local Information Link-state Topology (LILT) are introduced to deal with the dynamics of the mobile environment. Neither heuristic absolutely preserves connectivity, even if it is achievable in principle, i.e., the maximum powered graph  $G_{max}$  is connected.

Rodoplu and Meng [17] first conceived the idea of minimum energy mobile wireless networks. They allow nodes to set their transmission range much lower than the maximum, while keeping the network connected and maintaining minimum energy paths between each pair of nodes. Li and Halpern [5] improved their result by showing that nodes can start with a very small transmit power and incrementally search for a suitable value until all minimum energy paths are preserved. Their work produced similar results to [17], but with much lower overhead. Li and Wang [8] addressed the algorithmic complexity of the work in [17] and provided an algorithm with lower time complexity. Ahmed *et al.* [2] analyzed the minimum energy wireless network problem and proposed an improved algorithm for sparse networks.

Cone-Based Topology Control (CBTC), proposed by Li *et al.* [7], generates a graph structure similar to the one proposed by Yao in [24]. CBTC takes a parameter  $\alpha$  and each node determines a power level such that in every cone of degree  $\alpha$  within its surrounding area, there exists at least one node that is reachable using that power level. The connectivity of the produced subgraph depends on the value of  $\alpha$  and is only guaranteed when  $\alpha \leq 5\pi/6$ . A serious drawback of the algorithm is the need to decide on the suitable initial power level and the increment at each step. The choice of these two parameters may have a significant impact on the control message overhead to create the final topology.

Li *et al.* [9] propose a distributed topology control algorithm (called LMST) based on constructing minimum spanning trees. In-

stead of constructing global minimum spanning tree (MST), which requires global knowledge of the network topology, each node creates its own local minimum spanning tree among its neighbor set. While constructing such LMST, the weight of an edge is set to the necessary transmission power between its two ends. Once the local tree has been constructed, each node contributes to the final topology those nodes that are its neighbors in the local spanning tree. One problem with LMST is that the resulting graph does not preserve the minimum-energy paths.

For other related work in this area, Wattenhofer *et al.* [23] describe a two-phase algorithm, which consists of creating a variation of the Yao graph followed by a Gabriel Graph. The combined structure of Yao graph and Gabriel graph has been shown to be more sparse. Although these structures offer a constant bound on the energy stretch factor, they do not preserve minimum energy paths.

Although all of the above TC algorithms are very useful in practice, none of these provide any mathematical analysis to estimate the sparseness of topologies generated from the algorithms. Moreover, these TC algorithms do not ensure fault tolerance in their topologies. In this paper we provide a fault tolerant topology control protocol and present a detailed mathematical insight to derive sparseness of the topology generated by our algorithm.

There is recent research showing a tremendous interest in topology control as a means of interference reduction. However, the natural assumption that a sparse topology implies low interference was first refuted by Bukhart *et al.* [3]. They provide an intuitive definition of interference and, based on that definition, propose algorithms to construct connected subgraphs and spanners with minimum interference. Unfortunately, their solution does not preserve the minimum-energy paths between node pairs. Another algorithm, with the same drawback, is presented in [12], where the problem of minimizing the average or maximum interference (per link or node) is studied. Tang *et al.* [22] propose an algorithm for interference-aware topology control in multi-channel mesh networks based on IEEE 802.11 [4]. They provide a novel definition of co-channel interference and present efficient heuristics for channel assignment to the network such that the induced topology is interference-minimal. These issues, however, are beyond the scope of our paper.

### 3. PRELIMINARIES, ASSUMPTIONS AND ALGORITHM

In this section we present as background the distributed algorithm to construct minimum-energy path-preserving biconnected graph structures.

#### 3.1 Power model

We assume a generic, two-ray, wireless channel model, where the required transmission power is a function of distance [16]. To send a message from node  $s$  to node  $t$  separated by distance  $d(s, t)$  the minimum necessary transmission power is approximated by:

$$P_{s \rightarrow t} = K \times d^\alpha(s, t) \quad (2)$$

where  $\alpha \geq 2$  is the path loss factor, and  $K$  is a global constant. Here we assume symmetric channels. That is, if a node  $s$  can reach another node  $t$ , then  $t$  can also reach  $s$ . The power required for processing and receiving the signal are assumed to be negligible. The minimum power required to send from  $s$  to  $t$  using a node  $r$  as relay is:

$$P_{s \rightarrow r \rightarrow t} = P_{s \rightarrow r} + P_{r \rightarrow t} = K \times [d^\alpha(s, r) + d^\alpha(r, t)] \quad (3)$$

We also assume that each node is aware of its own position with reasonable accuracy, perhaps via GPS.

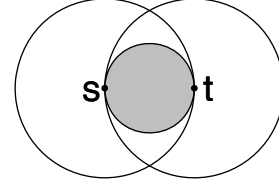


Figure 2: Cover region  $C(s, t)$  of node pair  $(s, t)$

#### 3.2 Minimum-energy path-preserving subgraphs

We say that a graph  $G' \subseteq G_{max}$  is a minimum energy path preserving graph or, alternatively, that it has the minimum energy property, if for any pair of nodes  $(u, v)$  that are connected in  $G_{max}$ , at least one of the (possibly multiple) minimum energy paths between  $u$  and  $v$  in  $G_{max}$  also belongs to  $G'$ . Minimum energy path preserving graphs were first defined in [5]. Typically, many minimum energy path preserving graphs can be formed from the original graph  $G_{max}$ . It has been shown that the smallest of such subgraphs of  $G_{max}$  is the graph  $G_{min} = (V, E_{min})$ , where  $(u, v) \in E_{min}$  iff there is no path of length greater than 1 from  $u$  to  $v$  that costs less energy than the energy required for a direct transmission between  $u$  and  $v$ . Let  $G_i = (V, E_i)$  be a subgraph of  $G_{max} = (V, E_{max})$  such that  $(u, v) \in E_i$  iff  $(u, v) \in E_{max}$  and there is no path of length  $i$  that requires less energy than the direct one-hop transmission between  $u$  and  $v$ . Formally  $G_{min}$  is:

$$G_{min} = \bigcap_{i=2}^{n-1} G_i \quad (4)$$

Any subgraph  $G'$  of  $G_{max}$  has the minimum energy property iff  $G' \supseteq G_{min}$ . Therefore, each of  $G_i$ , for any  $i = 2, \dots, n-1$  is a minimum energy path preserving graph because any of them is a supergraph of  $G_{min}$  by definition.

Among all  $G_i$ , the subgraph  $G_2$  can be efficiently constructed based on the 1-hop neighbor information because to construct  $G_2$ , we simply need to check all 2-length paths  $s \rightarrow r \rightarrow t$  between each node pair  $(s, t)$  where  $r$  is within the communication range of both  $s$  and  $t$ .

#### 3.3 Cover region

The algorithm presented in this paper is based on a concept called *cover region* introduced by Rahman *et al.* [14] which is described as follows. Consider a pair of nodes  $(s, t)$  such that the target  $t$  lies within the communication range of the source  $s$ . Envision the set of all points that can possibly act as relays between  $s$  and  $t$  such that it would be more power efficient for  $s$  to use an intermediate relay node  $r$  instead of sending directly to  $t$ . This set of points collectively forms the cover region of  $(s, t)$  pair. Mathematically:

$$\begin{aligned} C(s, t) &= \{ \langle x, y \rangle \mid P_{s \rightarrow \langle x, y \rangle \rightarrow t} \leq P_{s \rightarrow t} \} \\ &= \{ \langle x, y \rangle \mid K \times [d^\alpha(s, \langle x, y \rangle) + d^\alpha(\langle x, y \rangle, t)] \\ &\quad \leq K \times d^\alpha(s, t) \} \end{aligned}$$

Here we use  $\langle x, y \rangle$  to denote a hypothetical node located at position  $\langle x, y \rangle$ .

The shaded region of Figure 2 shows cover region  $C(s, t)$  for path loss factor  $\alpha = 2$ . Any node located in these shaded area can provide power savings if used as a relay to send from  $s$  to  $t$  (or from  $t$  to  $s$ ). The cover set of the same pair  $(s, t)$  in  $G_{max}$  is denoted by

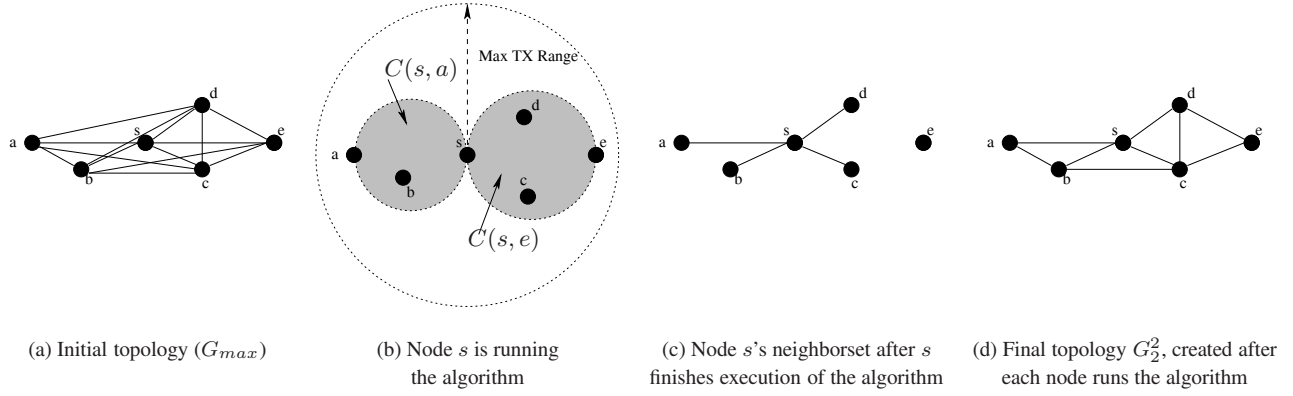


Figure 1: Illustrating construction of  $G_2^2$

$\xi_{G_{max}}(s, t)$  which is defined as:

$$\xi_{G_{max}}(s, t) = \{v | v \in V \wedge Loc(v) \in C(s, t)\}$$

The following lemma shows an important property of cover regions.

LEMMA 3.1. *Suppose the distance between  $s$  and  $t$  is  $d$ . For  $\alpha = 2$ , cover regions are circular regions centered at the midpoint on the straight line connecting  $s$  and  $t$ , and have radius  $d/2$ .*

PROOF. Without loss of generality, let us assume that  $s$  and  $t$  are located at  $(0, 0)$  and  $(d, 0)$ . Consider a hypothetical relay node  $r$  within the cover region of node pair  $(s, t)$  positioned at  $(x, y)$ . The power is saved when:

$$\begin{aligned} P_{s \rightarrow r} + P_{r \rightarrow t} &\leq P_{s \rightarrow t} \\ \Leftrightarrow K[x^2 + y^2 + (d-x)^2 + y^2] &\leq Kd^2 \end{aligned}$$

After some easy manipulations, the expression becomes:

$$\left(x - \frac{d}{2}\right)^2 + y^2 \leq \left(\frac{d}{2}\right)^2$$

which is the region confined within the circle centered at  $(d/2, 0)$ , and with radius  $d/2$ . Thus any relay node providing any power savings must fall within this circle.  $\square$

### 3.4 Articulation point

A vertex  $v$  in a connected graph  $G$  is an articulation point iff the deletion of vertex  $v$  together with all edges incident to  $v$  disconnects the graph into two or more nonempty components. A graph  $G$  is biconnected iff it contains no articulation points.

### 3.5 Minimum energy path preserving biconnected graphs

A graph  $G_2^2$  is a minimum energy path preserving biconnected graph iff it contains no articulation points and it keeps pairwise minimum energy paths. Formally,

DEFINITION 3.1. *A graph  $G_2^2 = (V, E_2^2)$  is a minimum energy path preserving biconnected subgraph of a biconnected graph  $G_{max} = (V, E_{max})$  iff  $E_2^2 \in E_{max}$  and  $G_2^2$  is biconnected and for each pair of  $(u, v) \in V$ , minimum energy paths between  $u$  and  $v$  in  $G_{max}$  are also in  $G_2^2$ .*

$G_2^2$  can be constructed by keeping all the edges  $(u, v) \in E_2^2$  iff  $(u, v) \in E_{max}$  and there exists at most one 2-length path requiring

less energy than the direct path  $(u, v)$ . Shortly,  $(u, v) \in E_2^2$  iff  $|\xi_{G_{max}}(u, v)| < 2$  where  $|\xi_{G_{max}}(u, v)|$  represents number of elements in  $\xi_{G_{max}}(u, v)$ . Such a graph can be constructed if a node knows the position of all 1-hop neighbors.

### 3.6 The Algorithm

In this section we describe distributed algorithms for constructing  $G_2^2$  topologies for a given topology  $G_{max}$ . As we are considering distributed algorithm, the following algorithms run at each node as per necessity. Consider a node  $s$  is constructing  $G_2^2$ . At

---

#### Algorithm 1 $updateCoverRegion(s, v)$

---

```

1: for each  $w \in N_{G_{max}}(s)$  do
2:   if  $Loc(v) \in C(s, w)$  then
3:      $\xi_{G_{max}}(s, w) = \xi_{G_{max}}(s, w) \cup \{v\}$ 
4:   else if  $Loc(w) \in C(s, v)$  then
5:      $\xi_{G_{max}}(s, v) = \xi_{G_{max}}(s, v) \cup \{w\}$ 
6:   end if
7:    $N_{G_{max}}(s) = N_{G_{max}}(s) \cup \{v\}$ 
8: end for
```

---



---

#### Algorithm 2 $G_2^2$ TOPOLOGY CONSTRUCTION

---

```

1: for each  $v \in N_{G_{max}}(s)$  do
2:   if  $|\xi_{G_{max}}(s, v)| < 2$  then
3:      $N_{G_2^2}(s) = N_{G_2^2}(s) \cup v$ 
4:   end if
5: end for
```

---

first  $s$  broadcasts a single *neighbor discovery message* (NDM) at the maximum power  $P_{max}$ . All nodes receiving the NDM from  $s$  send back a reply. While  $s$  collects the replies of its neighbors, it learns their identities and locations. It also constructs the cover sets with those neighbors. Initially, all those sets are empty. The set  $N_{G_{max}}(s)$ , which also starts with empty set, keeps track of all the nodes discovered in the neighborhood of  $s$  in  $G_{max}$ . Whenever  $s$  receives a reply to its NDM from a node  $v$ , it executes the algorithm  $updateCoverRegion(s, v)$  described in Algorithm 1.

After running  $updateCoverRegion(s, v)$ , node  $s$  executes Algorithm 2. For each neighbor  $v$  of  $s$  in  $G_{max}$  this algorithm checks whether number of nodes in the cover set is less than 2 or not. If the number of nodes in the cover set is less than 2 then  $v$  is included into the neighbor set of  $s$  in  $G_2^2$  since it indicates that we have at



most one node that can be used as relay to transmit message using lower energy than the direct path between  $s$  and  $v$ . Otherwise,  $v$  is not included into the neighbor set of  $s$  in  $G_2^2$ . It has been proven that topologies constructed this way preserve minimum energy paths and ensure biconnectivity [18].

**Example:** Let us consider the example scenario shown in Figure 1. The initial topology  $G_{max}$  is shown in Figure 1(a). Note that, all nodes are within the maximum transmission range of each other (i.e., reachable using maximum transmission power  $P_{max}$ ) except nodes  $a$  and  $e$ . Suppose node  $s$  is running the algorithm. At first, node  $s$  broadcasts a neighbor discovery message. All nodes receiving the broadcast send back a reply, one after another, announcing their existence and position. Suppose the first reply comes from node  $a$ . This is the first reply, so  $s$  sets  $\xi_{G_{max}}(s, a) = \emptyset$ . Next, suppose the reply from node  $b$  comes. From the position information appended in  $b$ 's reply, node  $s$  discovers that  $b$  is located on the cover region of node pair  $(s, a)$ , i.e., inside  $C(s, a)$  and node  $b$  should be included in the cover set of node pair  $(s, a)$ . Thus, it updates  $\xi_{G_{max}}(s, a) = \{b\}$  and sets  $\xi_{G_{max}}(s, b) = \emptyset$ . Then, suppose reply from node  $e$  arrives. It sets  $\xi_{G_{max}}(s, e) = \emptyset$ . When the reply messages from node  $c$  and  $d$  arrive later on, the cover set between node pair  $(s, e)$  gets updated as  $\xi_{G_{max}}(s, e) = \{c, d\}$  because  $Loc(c) \in C(s, e)$  and also,  $Loc(d) \in C(s, e)$ . The cover sets  $\xi_{G_{max}}(s, c)$  and  $\xi_{G_{max}}(s, d)$  remain  $\emptyset$ . In the final topology,  $s$  excludes node  $e$  from its direct neighbor set because  $|\xi_{G_{max}}(s, e)| = |\{b, c\}| = 2$ . However, it keeps  $a, b, c$ , and  $d$  in its direct neighbor set in  $G_2^2$  because the cardinality of cover sets with those nodes are less than 2, i.e.,  $|\xi_{G_{max}}(s, a)| = |\{b\}| = 1$ , and  $|\xi_{G_{max}}(s, b)| = |\xi_{G_{max}}(s, c)| = |\xi_{G_{max}}(s, d)| = |\emptyset| = 0$ . Thus, node  $s$ 's local connectivity with its neighbors becomes as shown in Figure 1(c). Ultimately the topology  $G_2^2$  is created (as shown in Figure 1(d)) once all of the nodes locally run the algorithm.

#### 4. ANALYTICAL MODEL

In this section, we develop mathematical model for determining structural density of  $G_2^2$ . Suppose  $n$  nodes are uniformly spread over a deployment area  $A$  in order to form a multi-hop wireless network. Thus, the average node density,  $\mu = \frac{n}{A}$ . Let us observe an arbitrary node  $s$  within this deployment area. Consider a hypothetical node  $t$  at distance  $x$  from  $s$ . Let us denote the probability of such node's existence by  $P_N(x)$ . Clearly  $P_N(x) = 0$ , if  $t$  is located outside the communication range of  $s$ . When  $x$  is located within the communication area,  $P_N(x)$  can be calculated as follows. Consider a small area strip defined by  $dx$  at the perimeter of the circle with radius  $x$  and centered at  $s$  as shown in Figure 3. Also consider a small angle  $d\theta$  measured from an arbitrary but fixed axis. The length of the arc  $\ell = xd\theta$  and the area of the small region  $dA$  within this small strip can be approximated as,  $dA = \ell dx = x dx d\theta$ . Therefore, the area of the entire small strip denoted by  $A_{strip}$  becomes,

$$A_{strip} = \int_0^{2\pi} dA = \int_0^{2\pi} \ell dx = \int_0^{2\pi} x dx d\theta = 2\pi x dx$$

Thus  $P_N(x)$  becomes:

$$\begin{aligned} P_N(x) &= \text{Area of the strip} \times \text{Node density} \\ &= A_{strip} \times \mu = 2\pi x dx \times \mu \\ &= 2\pi \mu x dx \end{aligned} \quad (5)$$

The probability of eliminating any node  $t$  from  $s$ 's neighbor set, denoted by  $P_E(x)$ , is the probability that there exists a neighbor  $t$  at distance  $x$  from  $s$  multiplied by its pruning probability  $P_P(x)$ .

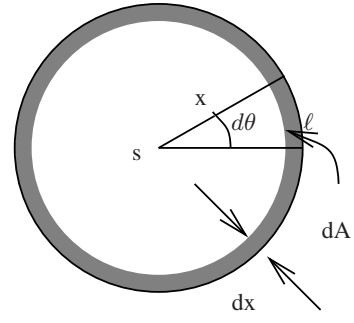


Figure 3: Illustrating a circular strip at distance  $x$

So  $P_E(x)$  becomes:

$$P_E(x) = P_N(x) \times P_P(x) = 2\pi \mu x dx \times P_P(x) \quad (6)$$

The expected number of neighbors eliminated by  $s$  from its neighbor set is found by integrating  $P_E(x)$  from 0 to the maximum transmission radius  $R$  within which  $s$  possibly can communicate:

$$\mathcal{T}_e = \int_0^R 2\pi \mu x \times P_P(x) dx \quad (7)$$

If we assume a disc communication area for  $s$  with radius  $R$  then the expected number of nodes within  $s$ 's maximum communication range becomes  $\pi R^2 \times \mu = \pi \mu R^2$ . Therefore, if we divide  $\mathcal{T}_e$  by  $\pi \mu R^2$ , we get the *average fraction of neighbors eliminated*,  $\mathcal{F}_e$ , which we define as *sparseness*,

$$\mathcal{F}_e = \frac{\mathcal{T}_e}{\pi \mu R^2} = \frac{\int_0^R 2\pi \mu x \times P_P(x) dx}{\pi \mu R^2} \quad (8)$$

Let's find the probability that a certain number of nodes  $k$  is located within the pruning region of the link  $\langle s, t \rangle$ . According to Lemma 3.1 the cover region of  $\langle s, t \rangle$  link is circular region with radius  $R = \frac{x}{2}$ . The probability that a node is placed in this circular area  $\pi R^2$  within the deployment area  $A = n/\mu$  is:

$$P_\Delta = \frac{\pi R^2}{A} = \frac{\pi R^2}{\frac{n}{\mu}} = \frac{\pi \mu x^2}{4n} \quad (9)$$

The probability  $P_k(C(s, t))$  that exactly  $k$  nodes are located in the pruning region  $C(s, t)$  is:

$$P_k(C(s, t)) = \binom{n-2}{k} P_\Delta^k \times (1 - P_\Delta)^{n-2-k} \quad (10)$$

Note that  $n - 2$  is used rather than  $n$  because we exclude  $s$  and  $t$ . For large  $n$  and small  $P_\Delta$ , the binomial distribution can be approximated using Poisson distribution [1], [11] with mean  $nP_\Delta$ . Thus,

$$P_k(C(s, t)) = \frac{(nP_\Delta)^k \times e^{-nP_\Delta}}{k!} \quad (11)$$

For constructing  $G_2^2$ , a link is pruned if there exists at least *two* nodes inside its cover region. Thus, the pruning probability be-

comes the probability that there exists two or more nodes in  $C(s, t)$ :

$$\begin{aligned}
P_P(x) &= \sum_{k=2}^n P_k(C(s, t)) \\
&= \sum_{k=2}^{\infty} \frac{(nP_{\Delta})^k \times e^{-nP_{\Delta}}}{k!} \\
&= e^{-nP_{\Delta}} \left( \sum_{k=0}^{\infty} \frac{(nP_{\Delta})^k}{k!} - \sum_{k=0}^1 \frac{(nP_{\Delta})^k}{k!} \right) \\
&= e^{-nP_{\Delta}} (e^{nP_{\Delta}} - 1 - nP_{\Delta}) \\
&= 1 - (nP_{\Delta} + 1) e^{-nP_{\Delta}} \quad (12)
\end{aligned}$$

By plugging in the value of  $P_{\Delta}$  from Equation 9 into Equation 12, we obtain:

$$P_P(x) = 1 - \left( 1 + \frac{\pi\mu x^2}{4} \right) e^{-\frac{\pi\mu x^2}{4}} \quad (13)$$

Finally, applying Equation 13 on Equation 7 we get:

$$\begin{aligned}
T_e &= \int_0^R 2\pi\mu x \times P_P(x) dx \\
&= 2\pi\mu \int_0^R x \left[ 1 - \left( 1 + \frac{\pi\mu x^2}{4} \right) e^{-\frac{\pi\mu x^2}{4}} \right] dx \\
&= 2\pi\mu \int_0^R x dx - 2\pi\mu \int_0^R x e^{-\frac{\pi\mu x^2}{4}} dx \\
&\quad - \frac{\pi^2\mu^2}{2} \int_0^R x^3 e^{-\frac{\pi\mu x^2}{4}} dx
\end{aligned}$$

The three integrals in the above equation can be separately solved as follows:

$$2\pi\mu \int_0^R x dx = \pi\mu R^2 \quad (14)$$

$$2\pi\mu \int_0^R x e^{-\frac{\pi\mu x^2}{4}} dx = -4 \left[ e^{-\frac{\pi\mu R^2}{4}} - 1 \right] \quad (15)$$

and,

$$\begin{aligned}
&\frac{\pi^2\mu^2}{2} \int_0^R x^3 e^{-\frac{\pi\mu x^2}{4}} dx \\
&= 2\pi\mu \int_0^R \left( \frac{\pi\mu x^2}{4} \right) e^{-\left( \frac{\pi\mu x^2}{4} \right)} x dx \quad (16)
\end{aligned}$$

Let  $\frac{-\pi\mu x^2}{4} = z$ . Thus,  $x dx = \frac{-2dz}{\pi\mu}$ . For  $x = 0$ , the new lower limit becomes  $z = 0$ , and for  $x = R$ , the new upper limit becomes,  $z = \frac{-\pi\mu R^2}{4}$ . Substituting these values into Equation 16, we get:

$$\begin{aligned}
&2\pi\mu \int_0^{\frac{-\pi\mu R^2}{4}} (-z) e^z \left( \frac{-2}{\pi\mu} \right) dz \\
&= 4 \int_0^{\frac{-\pi\mu R^2}{4}} z e^z dz \\
&= 4 \left[ (z - 1) e^z \right]_0^{\frac{-\pi\mu R^2}{4}} \\
&= 4 - (\pi\mu R^2 + 4) e^{-\frac{\pi\mu R^2}{4}} \quad (17)
\end{aligned}$$

**Table 2: Parameters used in simulation experiments**

Notation	Description	Value
$s$	speed of light	299792458 m/sec
$f$	operating frequency	2.4 GHz
$\lambda$	wave length	0.001605278 m
$h_t$	transmitting antenna height	1.5 m
$h_r$	receiving antenna height	1.5 m
$G_t$	transmitting antenna gain	1
$G_r$	receiving antenna gain	1
$L$	system loss	1
$r_{th}$	receiver sensitivity threshold	-68 dBm
$K$	propagation model constant	0.001605278

Finally, using Equations 14, 15, and 17 and performing some manipulations we get:

$$T_e = \pi\mu R^2 - 8 + (\pi\mu R^2 + 8) e^{-\frac{\pi\mu R^2}{4}} \quad (18)$$

Therefore, using Equation 18 and Equation 8, we get:

$$F_e = \frac{\pi\mu R^2 - 8 + (\pi\mu R^2 + 8) e^{-\frac{\pi\mu R^2}{4}}}{\pi\mu R^2} \quad (19)$$

According to Equation 19, the sparseness,  $F_e$  is a function of two network parameters namely, maximum transmission range ( $R$ ), and node density ( $\mu$ ), i.e.,  $F_e = f(R, \mu)$ . The general effects of these parameters (while changing one and keeping the other fixed) are as follows:  $F_e$  increases when either  $R$  or  $\mu$  is increased.

## 5. SIMULATION EXPERIMENTS

In this section, we present simulation results to verify the accuracy of our analytical model.

### 5.1 Simulation environment

#### 5.1.1 Radio parameters:

We assume that each node has an omni-directional antenna with 0 dB gain located 1.5 meter above the node. The path-loss exponent,  $\alpha = 2$ . The carrier frequency is 2.4 GHz (the operating frequency of IEEE 802.11g networks). The speed of light is assumed to be  $3 \times 10^8$  m/sec which gives us a wavelength  $\lambda = 0.001605278$ m. The received signal strength threshold to ensure radio connectivity between nodes is set to -68 dBm<sup>1</sup>. Table 2 summarizes all the parameters that have been used for simulation experiments. Given these parameters, the value of  $K$  for the Equation 2 and 3 becomes 0.001605278 and the cross over distance becomes:

$$d_{cross} = \frac{4\pi h_t h_r}{\lambda} = 226.44m$$

As the path loss factor  $\alpha$  was set to 2, the *maximum* transmission range ( $R_{max}$ ) was restricted below the cross over distance and set to  $R_{max} = 225$ m. *Minimum* transmission range was set to 125m for all simulation experiments.

#### 5.1.2 Scenarios

We simulate randomly deployed networks of 100, 300, and 500 nodes over a  $625m \times 625m$  square region. Thus, the node density was varied by changing number of nodes over a fixed deployment region. We only consider connected networks, since it is not

<sup>1</sup>we note that commercially available LinkSys routers with WRT150N series has the similar receiver sensitivity threshold

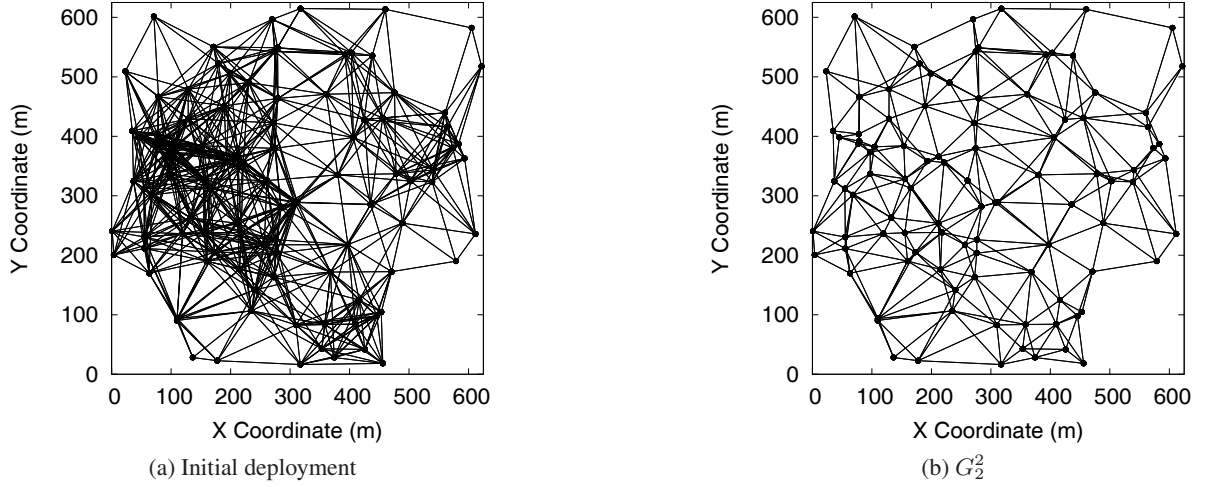


**Figure 4: Illustrating an example scenario of 100 nodes deployed over a  $625\text{m} \times 625\text{m}$  square area. TX range is 150m**

possible to generate *connected* sub-networks  $G_2^2$  unless the initial networks are connected. For each network size we have generated 10 scenarios. Performance measures are reported as an average of these 10 random samples.

### 5.1.3 Performance metric

We analyze the performance of  $G_2^2$  using *sparseness* as a metric. The number of links remaining in a  $G_2^2$  subgraph determines its sparseness. Thus, the sparseness of a network is determined by measuring the average fraction of eliminated neighbors,  $F_e$ .

The degree of sparseness of a network has a major impact on routing performance of the routing layer. For instance, *flooding*, if used for route discovery, is known to create serious *broadcast storm problem* in a dense graph [19]. By reducing neighbor set of each node, this problem can be mitigated to some extent. Moreover, in a sparse topology, the average path length is relatively large (increasing end-to-end delay), and the number of vertex-disjoint paths between pair of nodes is relatively small (reducing fault-tolerance).

## 5.2 Results

### 5.2.1 Numerical example

Figure 4(a) shows an example scenario of 100 nodes randomly deployed over a  $625\text{m} \times 625\text{m}$  square area. The transmission range was set to  $150\text{m}$ . The initial topology contains 834 links in total. We determine the one hop neighborset of each node based on this initial topology. Then, each node runs the algorithm to construct  $G_2^2$  (i.e., Algorithm 2) and determines the fraction of neighbors eliminated from its (one hop) neighborset. Finally we take the average of each node's fraction of eliminated neighbors to determine the actual value of  $F_e$ . Figure 4(b) shows the topology generated from the algorithm. The value of  $F_e$  was found to be 52.27% in this topology. Now, let us apply Equation 19 to the example scenario shown in Figure 4(a). The deployment area  $A = 625\text{m} \times 625\text{m} = 390625\text{ m}^2$  and  $n = 100$  result in a node density  $\mu = n/A = 100/390625 = 0.000256$ . Transmission radius  $R = 150\text{m}$ . So,

$$\pi\mu R^2 = 3.1428 \times 0.000256 \times (150)^2 = 18.1025$$

With such parameter values, Equation 19 gives us,

$$\begin{aligned} F_e &= \frac{\pi\mu R^2 - 8 + (\pi\mu R^2 + 8) e^{-\frac{\pi\mu R^2}{4}}}{\pi\mu R^2} \\ &= \frac{18.1025 - 8 + (18.1025 + 8) e^{-\frac{18.1025}{4}}}{18.1025} \\ &= 0.573 \end{aligned}$$

Therefore,  $F_e = 57.3\%$  for  $G_2^2$ . Thus the analytical expression gives us a value very close to what we obtained using the simulation experiment (with a deviation of around 5%).

### 5.2.2 Effect of transmission range

To see the effect of transmission range on sparseness, we measure  $F_e$  for  $G_2^2$  with different node densities. The transmission range is varied between  $125\text{m}$  to  $225\text{m}$  with an increment of  $25\text{m}$  at each step. Figure 5 shows the result. Measurements from both simulation experiments and analytical expressions are plotted in the same graph for a fair comparison. As can be seen from the figure,  $F_e$  exponentially increases with the increase in transmission range. Also for all scenarios, the results of analytical expressions are very close to the simulation results; the difference is very small, maximal being around 6.5%. Thus, the analytical models are effectively able to capture the generic pattern of the simulation results. The small inaccuracy arises from the nodes located close to the boundaries of the deployment region, for which the communication area is restricted, and thus they have fewer neighbors. With larger transmission ranges the effect also becomes larger. We ignored this "boundary effects" to simplify the analytical models.

### 5.2.3 Effect of node density

Finally, we present the effect of node density on the sparseness. Node density were varied by varying number of nodes between  $100 - 500$  while keeping the deployment region constant. Figure 6 shows the sparseness for  $G_2^2$  under three transmission radius  $225\text{m}$ ,  $175\text{m}$  and  $125\text{m}$ . The result is as expected: a higher fraction of neighbors is eliminated in more dense networks for all transmission ranges. With larger node densities, it is highly probable that the required number of nodes exist in the cover region of a link, and the link gets pruned by the algorithm.

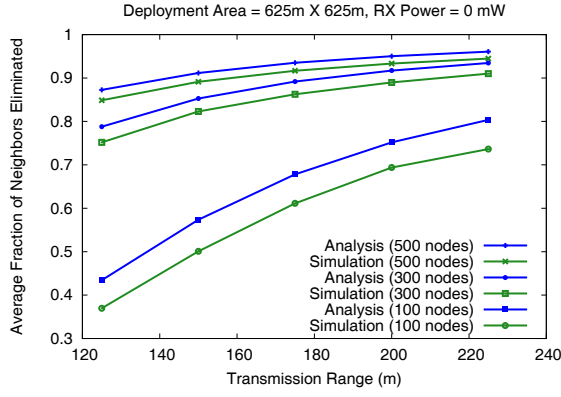


Figure 5: Effect of transmission range on  $G_2^2$

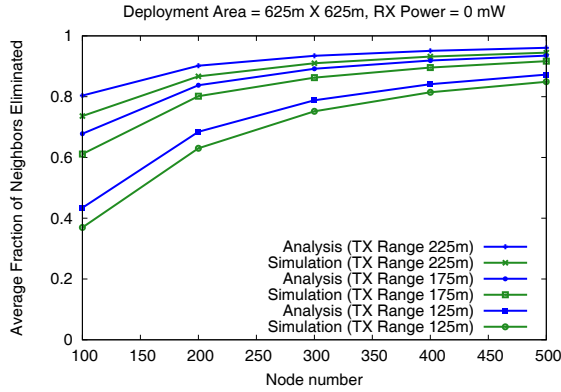


Figure 6: Effect of node density on  $G_2^2$

## 6. CONCLUSIONS AND FUTURE WORK

We have presented analytical model to determine structural densities of topologies generated by a minimum energy path preserving biconnected TC algorithm. Using this model, the network designer can easily estimate the network structure for the desired topology prior to network deployment.

There are several ways to extend this work. The analytical expression is developed for the path loss factor  $\alpha = 2$  and under the assumption that nodes are uniformly distributed over the deployment area. This expression can be further generalized for other values of path loss factor and other node distributions.

## 7. REFERENCES

- [1] Poisson distribution.  
[http://en.wikipedia.org/wiki/Poisson\\_distribution](http://en.wikipedia.org/wiki/Poisson_distribution).
- [2] M. Ahmed, M. Shariar, S. Zerín, and A. Rahman. Analysis of minimum-energy path-preserving graphs for ad-hoc wireless networks. In *Symp. on Perform. Eval. of Comp. and Telecomm. Sys.*, June 2008.
- [3] M. Burkhart, P. V. Rickenbach, R. Wattenhofer, and A. Zollinger. Does topology control reduce interference? In *MobiHoc*, 2004.
- [4] I. S. Department. Wireless LAN medium access control (MAC) and physical layer (PHY) specifications, 1997. IEEE standard 802.11-1997.
- [5] L. Li and J. Halpern. Minimum energy mobile wireless networks revisited. In *Proceedings of IEEE ICC*, 2001.

- [6] L. Li and J. Y. Halpern. A minimum-energy path-preserving topology-control algorithm. *IEEE Trans. on Wire. Comm.*, 3(3):910–921, 2004.
- [7] L. Li, J. Y. Halpern, P. Bahl, Y. Wang, and R. Wattenhofer. Analysis of a con-based topology control algorithm for wireless multi-hop networks. In *ACM Symp. on Principle of Dist. Computing (PODC)*, 2001.
- [8] M. Li, Y. Wang, and W.-Z. Song. Applications of k-local mst for topology control and broadcasting in wireless ad hoc networks. *Parallel and Distributed Systems, IEEE Transactions on*, 15(12):1057–1069, 2004.
- [9] N. Li, J. C. Hou, and L. Sha. Design and analysis of an MST-based topology control algorithm. In *Proceedings of INFOCOM*, 2003.
- [10] J. Lin, X. Zhou, and Y. Li. A minimum-energy path-preserving topology control algorithm for wireless sensor networks. *International Journal of Automation and Comp.*, 6:295–300, 2009.
- [11] B. Milic and M. Malek. Dropped edges and faces’ size in gabriel and relative neighborhood graphs. *IEEE MASS*, 0:407–416, 2006.
- [12] K. Moaveninejad and X. Li. Low-interference topology control for wireless ad hoc networks. *AHSN*, 1(1-2), 2005.
- [13] J. P. Monks, V. Bhargavan, and W. M. Hwu. A power controlled MAC protocol for wireless packet networks. In *Proceedings of INFOCOM*, pages 219–228, 2001.
- [14] A. Rahman and P. Gburzynski. MAC-assisted topology control for ad-hoc wireless networks. *Int. J. Commun. Syst.*, 19(9):955–976, 2006.
- [15] R. Ramanathan and R. Rosales-Hain. Topology control of multihop wireless networks using transmit power adjustment. In *In Proc. of IEEE INFOCOM 2000*, pages 404–413, Tel Aviv, Israel, March 2000.
- [16] T. Rappaport. Wireless communications: principles and practice, 1996.
- [17] V. Rodoplu and T. Meng. Minimum energy mobile wireless networks. *IEEE Journal on Sel. Areas in Comm. (JSAC)*, 17(8):1333–1344, 1999.
- [18] H. Roy, S. K. De, M. Maniruzzaman, and A. Rahman. Fault-tolerant power-aware topology control for ad hoc wireless networks. In *IFIP NETWORKING*, 2010.
- [19] Y.-S. C. h. S.-Y. Ni, Y.-C. Tseng and J.-P. Sheu. The broadcast storm problem in a mobile ad hoc network. In *Mobicom*, 1999.
- [20] S. Singh and C. Raghavendra. Power efficient MAC protocol for multihop radio networks. In *Proceedings of PIMRC*, pages 153–157, 1998.
- [21] S. Singh, M. Woo, and C. Raghavendra. Power-aware routing in mobile ad hoc networks. In *Proceedings of MobiCom*, pages 181–190, 1998.
- [22] J. Tang, G. Xue, and W. Zhang. Interference-aware topology control and QoS routing in multi-channel wireless mesh networks. In *Proceedings of ACM MOBIHOC*, pages 68–77. ACM Press, 2005.
- [23] R. Wattenhofer, L. Li, P. Bahl, and Y.-M. Wang. Distributed topology control for wireless multihop ad-hoc networks. In *INFOCOM*, 2001.
- [24] A. Yao. On constructing minimum spanning trees in  $k$ -dimensional spaces and related problems. *SIAM Journal on Comp.*, 1982.